PHYSICAL REVIEW B **80**, 024419 (2009)

Spin-glass behavior in $LuFe_2O_{4+\delta}$

Fan Wang, Jungho Kim, and Young-June Kim*
Department of Physics, University of Toronto, Toronto, Ontario, Canada M5S 1A7

G. D. Gu
Department of Condensed Matter and Material Science, Brookhaven National Laboratory, Upton, New York 11973, USA
(Received 12 December 2007; revised manuscript received 28 April 2009; published 21 July 2009)

We have carried out a comprehensive investigation of magnetic properties of $LuFe_2O_{4+\delta}$, measuring ac susceptibility, dc magnetization, and specific heat. A magnetic phase transition around 236 K is identified as a paramagnetic to ferrimagnetic transition in accordance with previous studies. Upon further cooling below this temperature, highly relaxational magnetic behavior is observed: the dc magnetization exhibits history and time dependence, and the real and the imaginary parts of the ac susceptibility show large frequency dependence. Dynamic scaling of the ac susceptibility data suggests that this low-temperature phase can be described as a spin-glass phase. We also discuss the magnetic field dependence of the spin-glass transition and aging, memory, and rejuvenation effect below the glass transition temperature around 229 K.

DOI: 10.1103/PhysRevB.80.024419 PACS number(s): 75.50.Lk, 75.50.Gg, 75.40.Cx, 75.40.Gb

I. INTRODUCTION

Geometrical frustration plays an important role in determining ground states and phase transitions in magnetic systems. A triangular lattice in two dimensions in particular is one of the simplest systems to study the effect of geometrical frustration. $LuFe_2O_4$ (LFO) is a member of RFe_2O_4 family of compounds, where R can be Y, Ho, Er, Tm, Yb, and Lu.[1] All these materials have hexagonal layered structure, in which Fe ions form a triangular lattice within each bilayer.[2] Since the average charge valence of Fe in this compound is +2.5, this system is expected to exhibit charge order behavior similar to Fe_3O_4 (Refs. 3 and 4) or half-doped manganites.[5] However, due to the geometrical frustration introduced by the triangular lattice, understanding charge order in this material is not straightforward.[6] Previous electron and x-ray diffraction studies have shown that charge ordering sets in below ~300 K, and anomalous dielectric dispersion was observed in this temperature range.[6,7] In particular, Ikeda *et al.* argued that the observed pyroelectric signal below charge ordering temperature indicates charge order driven ferroelectricity.[7] This result has been drawing much attention[8,9] since it would be the first such observation of ferroelectricity originating from charge ordering. In addition, it was observed that the pyroelectric signal shows an unusual step around 250 K which is very close to the spin ordering temperature of ~240 K.[10,11] Large magnetodielectric response under low magnetic fields was also observed in $LuFe_2O_4$ at room temperature,[12] which prompted further interest in this compound as a possible multiferroic (or magnetic ferroelectric) material.[13]

Although whether the magnetic and the ferroelectric order parameters are coupled in $LuFe_2O_4$ is not clear at the moment, $LuFe_2O_4$ exhibits quite interesting magnetic properties. Strong antiferromagnetic interaction exists between the nearest spins on a triangular net[10,11,14] and as a result geometrical spin frustration exists. Most earlier studies of the magnetism in RFe_2O_4 have been focused on YFe_2O_4. Tanaka *et al.* first reported that the Fe spins order below 220 K based on their Mössbauer experiments.[15] In their studies of transport properties, they also observed that there are two distinct transitions at 240 and 225 K, and the former corresponds to Verwey-like charge ordering accompanied by magnetic ordering.[16] This was corroborated in the x-ray study of Nakagawa *et al.*, and two first-order structural transitions were found at ~230 and 190 K corresponding to transitions from hexagonal to monoclinic and then to triclinic, respectively.[17] Recently, Ikeda *et al.* reported that there are at least five different phase transitions below 225 K in YFe_2O_4 based on their x-ray powder-diffraction studies.[18]

However, it was also realized that the oxygen nonstoichiometry in YFe_2O_4 can cause significant changes in its magnetic properties, while $LuFe_2O_4$ is believed to be free from such oxygen nonstoichiometry problems.[19] In their comprehensive magnetization and neutron scattering work on $LuFe_2O_4$, Iida *et al.* were able to elucidate unusual magnetic properties of this compound.[14] Specifically, they found that the system does not show any long-range three-dimensional (3D) magnetic order down to 4.2 K. Instead, they argued that the system at low temperature consists of ferrimagnetic clusters of various sizes, based on their thermoremanent magnetization measurements. The ferrimagnetism in this case arises due to the mixture of $S=2$ and $S=5/2$ spins. In recent neutron-scattering experiments, however, sharp magnetic Bragg peaks were observed, suggesting the existence of long-range magnetic order.[11] Therefore, the nature of the magnetic ground state of $LuFe_2O_4$ seems to vary depending on the sample preparation. Indeed, we found that the oxygen nonstoichiometry in $LuFe_2O_4$ affects its ground-state property significantly.

In this paper, we report our comprehensive study of magnetic properties of $LuFe_2O_{4+\delta}$ (excess oxygen) using ac susceptibility, dc magnetization, and specific heat. We have observed two magnetic transitions: the high-temperature transition occurs at ~237 K and corresponds to the previously observed ferrimagnetic transition.[10,11,14] The signature of this transition is also observed in our specific-heat measurements. In addition to this ferrimagnetic transition, we

observe an unusual magnetic transition at a lower temperature, which shows relaxational behavior similar to that of a spin-glass (SG) phase.

This paper is organized as follows. In the next section, we will explain our sample preparation and characterization in detail. In Sec. III, our experimental results from magnetic susceptibility and specific-heat measurements are presented. In Sec. IV, we will discuss the implication of the observed results and the possible connection with the charge order and ferroelectricity.

II. EXPERIMENTAL DETAILS

LFO single crystals were grown using the traveling solvent floating zone method at Brookhaven National Laboratory following the method reported in Ref. 20. Our experiments were done using the crystals from the same batch without any special annealing procedure. The chemical composition of one of the crystals was examined with electron probe microanalysis with beam size less than 1 μm. The Lu/Fe ratio was analyzed at 25 randomly selected points on the sample surface. The average Lu/Fe ratio was 1.98 ± 0.02, which shows that Lu and Fe are homogeneously distributed with almost stoichiometric ratio. We found out that the magnetic and structural properties of $LuFe_2O_{4+\delta}$ varies widely among the as-grown samples due to oxygen nonstoichiometry.[11] The oxygen contents of two pieces exhibiting different magnetic behavior were studied using thermogravimetric analysis (TGA). The samples were heated in reducing atmosphere (5% H_2:Ar) up to about 1025 °C, at which temperature the LFO sample decomposes into Lu_2O_3 and Fe. The oxygen concentration of the sample showing magnetic properties reported here is 4.07 ± 0.03, while the other sample has less oxygen content and is close to stoichiometric value of 4. Detailed study of phase diagram is still in progress, but the rest of this work is based on the study of $\delta = 0.07$ sample, which has a rectangular parallelepiped shape ($3 \times 3 \times 1$ mm). dc magnetization and ac susceptibility measurements were done using Quantum Design superconducting quantum interference device magnetometer. Specific-heat measurements on the same sample were carried out using the thermal relaxation method on Quantum Design Physical Property Measurement System (PPMS).

III. EXPERIMENTAL RESULTS

A. dc magnetization

In Fig. 1(a), we show the temperature dependence of the thermomagnetization of $LuFe_2O_4$ obtained with 10 Oe field applied parallel to the crystallographic c axis which is perpendicular to the hexagonal planes. A sharp peak appears in the magnetization curve at a temperature of ~237 K, below which the field-cooled data begin to diverge from the zero-field-cooled (ZFC) data. In Fig. 1(b), thermomagnetization obtained in a field perpendicular to the c axis is shown. Note that the magnetization in this direction is two orders of magnitude smaller than that shown in panel (a). The possible sample misalignment with respect to the field direction, which is less than 1°, can entirely account for this small

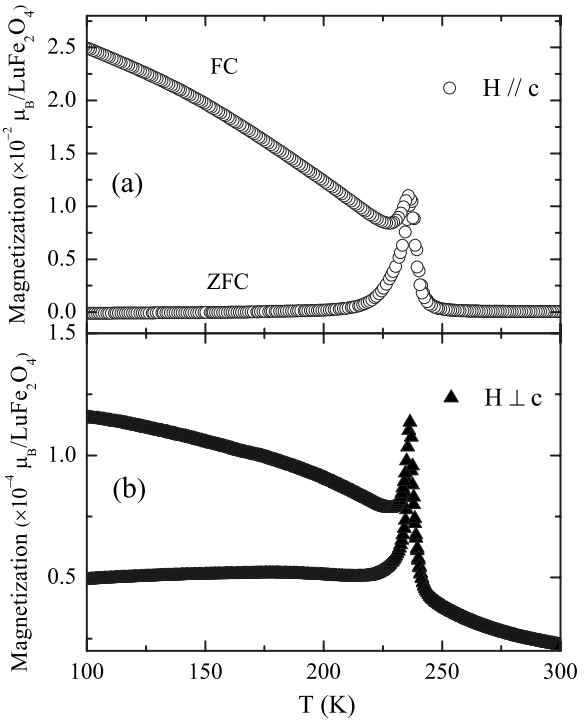

FIG. 1. Temperature dependence of magnetization measured with 10 Oe field applied (a) parallel and (b) perpendicular to the c axis, respectively.

magnetization. This also illustrates that the easy axis is along the c axis and the Ising anisotropy is very large. The nonzero ZFC magnetization at low temperature in this case is probably due to the small residual field in the magnetometer. This peak at 237 K was also observed in dc magnetization by Iida *et al.*,[14] which is ascribed to the formation of ferrimagnetic clusters. Recent neutron-scattering experiments showed that long-range ferrimagnetic order forms below the temperature of dc magnetization peak,[10,11] indicating that the peak observed here comes from the ferrimagnetic ordering.

B. Specific heat

Figure 2 shows the temperature dependence of the specific heat, $C(T)$, of the same sample used in the magnetization study. One can identify two features in this curve. The high-temperature feature above 300 K is relatively broad and has a maximum at ~330 K. This feature is related to the 3D charge order observed in previous electron and x-ray diffraction studies.[6] The low-temperature peak emerges below ~250 K and has a cusp at ~237 K. The peak position of this low-temperature feature is very close to the peak in magnetic susceptibility, suggesting that this feature is related to the ferrimagnetic phase transition.

C. ac susceptibility

Figure 3 shows the real and imaginary parts of the ac susceptibility as a function of temperature. The different curves correspond to data obtained with different driving frequencies. The amplitude of the ac field was kept constant at

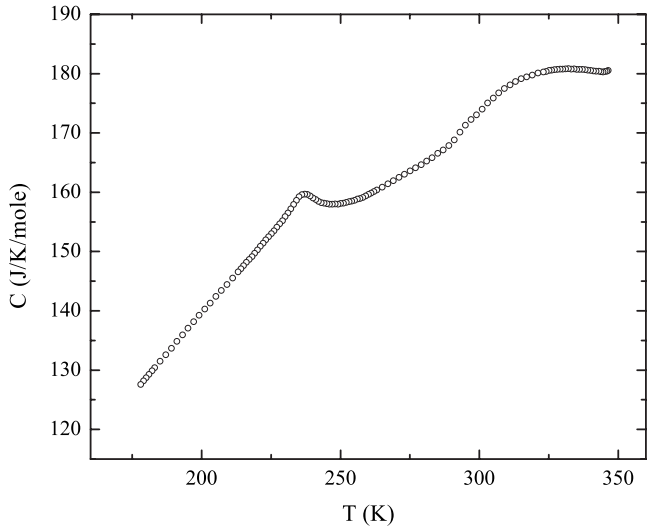

FIG. 2. Temperature dependence of heat capacity $C(T)$ measured on continuous cooling.

$h_{ac}=1$ Oe. A well-defined peak is observed for the real part of the susceptibility χ' at 237 K and the low-temperature tail of this peak decreases with increasing frequency. The imaginary part of the susceptibility, χ'', appears below ~240 K and consists of two peaks. The high-temperature component,

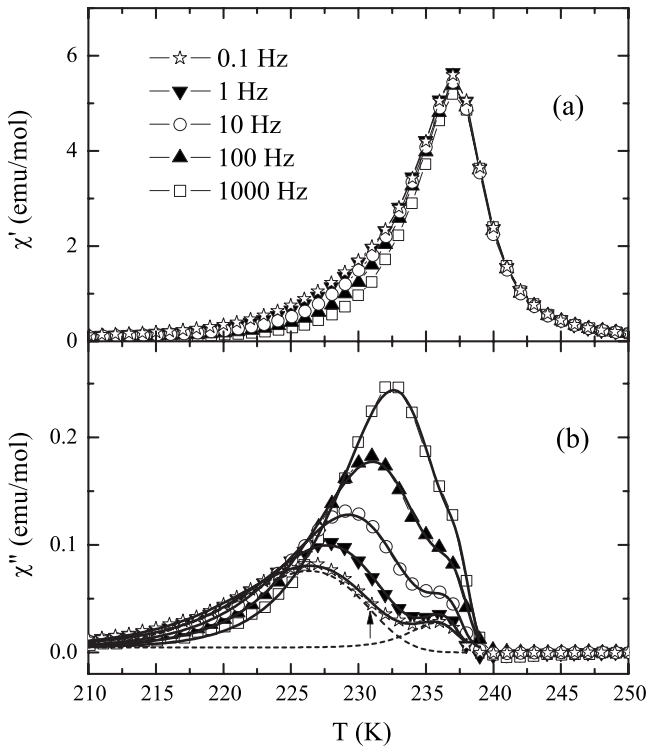

FIG. 3. Temperature dependence of the ac magnetic susceptibility obtained with different frequencies as labeled. ac field with amplitude $h_{ac}=1$ Oe was applied and the magnetization was measured. The real and the imaginary parts of the susceptibility are shown in parts (a) and (b), respectively. The solid lines in part (b) are the fitting results as described in the text. For the 0.1 Hz data, individual components are shown as dashed lines and the inflection point is noted with an arrow.

appearing as a shoulder, is located at ~237 K and grows as the frequency increases, while the peak position remains the same. This shoulder position is almost the same as the peak position of the dc magnetization, suggesting the ferrimagnetic origin of this component. On the other hand, the low-temperature peak grows and shifts to higher temperature with increasing frequency. Such a frequency dependence of ac susceptibility is commonly observed in spin-glass systems. For a spin-glass system, the spin dynamics become sluggish with decreasing temperature, so that it takes longer time for a spin to relax and the maximum relaxation time increases accordingly. When an external ac magnetic field with a driving frequency $\omega/2\pi$ is applied to a spin-glass system, if the maximum relaxation time $\tau_{\max}$ is longer than $2\pi/\omega$, the system will not be able to keep up with the oscillating field and becomes out of equilibrium. Therefore, one can define the freezing temperature, T_f, as the temperature at which $\tau_{\max}=2\pi/\omega$. As a result, T_f is a function of driving frequency ω. Experimentally $T_f(\omega)$ can be determined from the maximum of $\chi'(\omega)$, while sometimes the inflection point of $\chi''(\omega)$ is used to determine T_f in the case when the peak in $\chi'(\omega)$ is not clear. Both methods have been widely used in finding T_f in SG systems.[21–23] Since the maximum of χ' is difficult to identify in our system due to the second peak located at 237 K, we use the imaginary part $\chi''(\omega)$ which shows a double-peak feature. Two asymmetric peaks were used to fit $\chi''(\omega)$, and T_f could be extracted from the inflection point of the low-temperature peak. The fitting function used in our analysis is a purely empirical form $\sim\exp(-e^x+x)$ with $x\equiv\frac{T-T_0}{W_0}$, where T_0 and W_0 denote the peak position and the width.[24]

The maximum relaxation time and $T_f(\omega)$ can be modeled with conventional critical slowing down[25]

$$\tau_{\max}=\tau_0(T_f/T_g-1)^{-z\nu}, \tag{1}$$

where T_g is the spin-glass transition temperature, z is the dynamical exponent, ν is the usual critical exponent for the correlation length, and τ_0 is the microscopic flipping time of the fluctuating spins. The dynamic scaling of the ac susceptibility is shown in Fig. 4, and the best fit to Eq. (1) yields $T_g=229\pm1$ K, $z\nu=6.9\pm1.8$, and $\tau_0=10^{-13.0\pm2.0}$ s. The value of τ_0 is very close to the microscopic spin-flip time $\sim10^{-13}$ s in other spin-glass systems.[21–23,26] The value of $z\nu$ is within the range of well-known spin glasses such as CuMn (4.6 at. %) ($z\nu=5.5$) (Ref. 27) and $CdCr_2(In)S_4$ ($z\nu=7$).[28] This value of $z\nu$ is also close to the value obtained from numerical simulations in 3D Ising spin glasses.[29–31] Due to the existence of high-temperature peak, it is difficult to extract T_f for high-frequency data, which result in large error bars. However, the observed scaling behavior is consistent with canonical spin-glass behavior and indicates that the low-temperature phase is quite possibly a spin-glass phase. Thus, taken together with the heat capacity and the susceptibility data, LFO seems to undergo a continuous phase transition from a Curie paramagnetic phase to a ferrimagnetic phase at ~237 K and then to a spin-glass phase below 229 K. It is not clear at the moment whether the magnetic order disappears in the spin-glass phase.

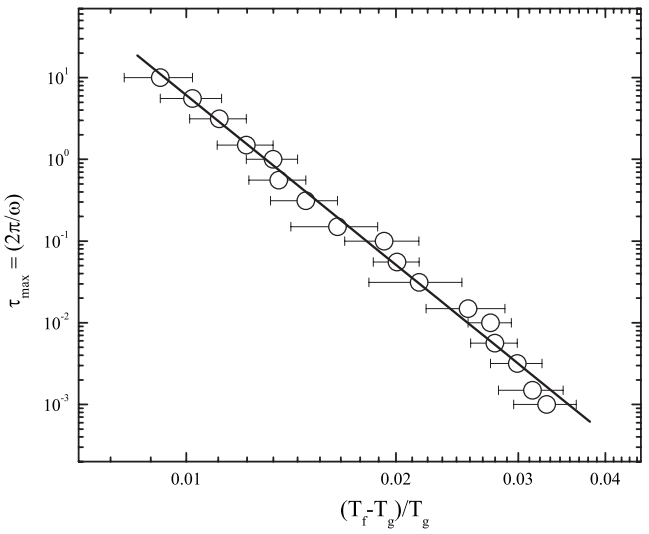

FIG. 4. Dynamic scaling of the reduced temperature vs $\tau_{\max}(T_f)=2\pi/\omega$ in a log-log scale. The solid line is Eq. (1) with $z\nu=6.9$, $\tau_0=1\times10^{-13}$ s, and $T_g=229$ K.

D. Nonequilibrium phenomena

Although spins are considered "frozen" in the spin-glass phase, the system in fact simply does not reach the equilibrium state within the experimental time scale due to the slow dynamics. As a result, spin-glass systems exhibit nonequilibrium phenomena. One such example is aging. When a spin-glass system is cooled below T_g, the domains begin to grow logarithmically in time, and the relaxation rate can be defined as $S\equiv(1/H)\partial M/\partial\log(t)$.[32] In Fig. 5, we show $S(t)$ as a function of $\log_{10}(t)$. Note that the sample was cooled down to $0.87T_g\sim200$ K in the absence of magnetic field. After waiting for a certain amount of time ($t_w=1000$, 5000, and 10 000 s) without external field, the magnetization was recorded as a function of time with 10 Oe magnetic field applied. As can been seen from the figure, t at which the maximum relaxation rate occurs increases with increasing t_w and in fact it is almost equal to t_w. This kind of aging behavior illustrates nonequilibrium dynamics of domain growth and is commonly observed in other spin-glass systems.[22,33]

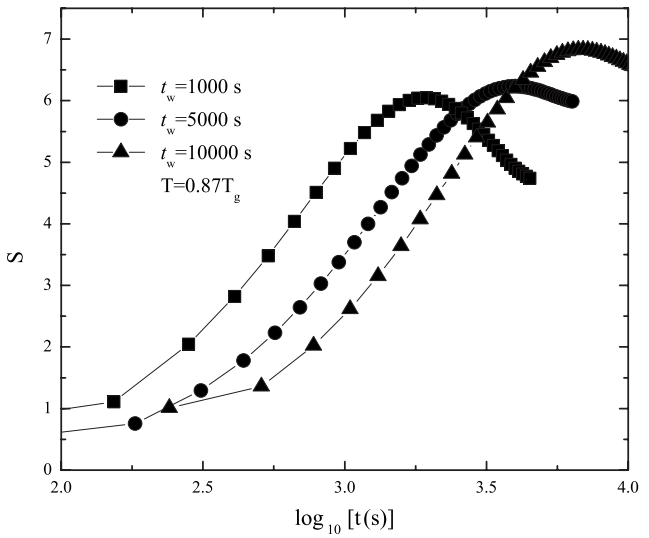

FIG. 5. Relaxation rate S defined in the text is plotted as a function of $\log_{10}(t)$ at $T=0.87T_g$ ($T_g=229$ K). Each curve is obtained by measuring at $H=10$ Oe after waiting for t_w following the cool down.

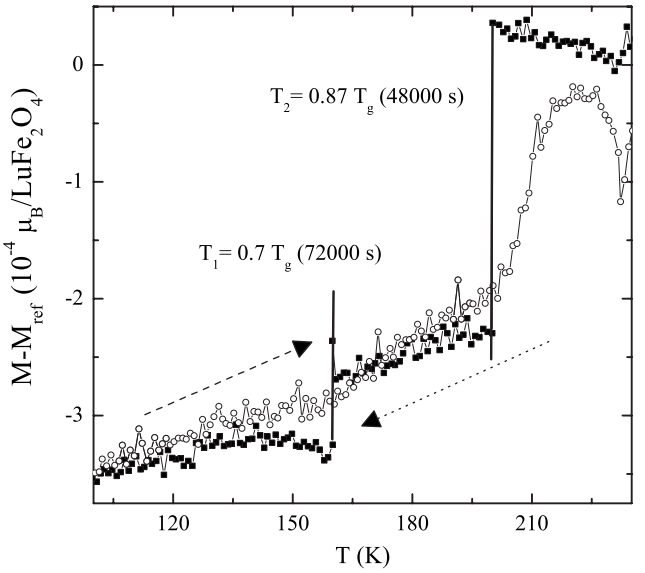

FIG. 6. The relative magnetization M-M_{ref} is plotted as a function of temperature. The magnetization measured on continuous cooling in $H=10$ Oe field is plotted as solid symbols. During the cooling, there were two halts at $T_1=0.7T_g$ and $T_2=0.87T_g$ ($T_g=229$ K). The open symbols denote the measurements done on reheating. The reference M_{ref} was obtained by continuously cooling and reheating in 10 Oe. The cooling and heating rates in both measurements were 2 K/min.

Another interesting example of nonequilibrium dynamics of spin-glass system is the so-called memory effect. In order to show this effect, we have measured temperature dependence of $M(T)$ in two distinct routes. The first, M_{ref}, was obtained by cooling in 10 Oe magnetic field from 300 K down to 50 K at a constant cooling rate of 2 K/min and then heating back continuously at the same rate. In the second route, M was recorded on cooling in 10 Oe at the same rate from 300 to 50 K with two halts at $T_1=160$ K for 72 000 s and at $T_2=200$ K for 48 000 s. During the halts, the external field is turned off to let the magnetization relax. After each halt, M shows a clear deviation from the reference as illustrated in Fig. 6 due to aging. After reaching 50 K, the sample temperature is increased continuously at 2 K/min rate in $H=10$ Oe. During the reheating, the system exhibits a steplike feature at both T_1 and T_2. The jump at T_1 is not very pronounced but clear jump in $M(T)$ around T_2 is clearly visible. This suggests that the system somehow remembers the history of halts during cooling. Exceeding the halt points, M recovers to the reference value and the system is called rejuvenated. Such aging, memory, and rejuvenation behaviors were observed in other spin-glass systems as well.[26,34,35] These observations also suggest that the low-temperature phase of LFO is consistently described as a spin glass.

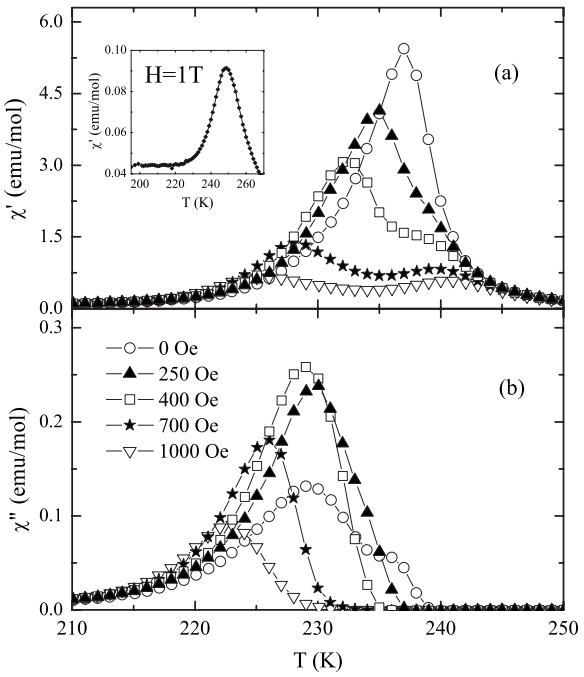

FIG. 7. (a) The real and (b) the imaginary parts of ac magnetic susceptibility versus temperature. The driving frequency was fixed at $\omega/2\pi=10$ Hz and $h_{ac}=1$ Oe. Each curve was obtained under different applied static magnetic field of H. The inset shows the data obtained with $H=1$ T.

E. Magnetic field dependence

In Fig. 7, ac susceptibility at 10 Hz driving frequency is plotted as a function of temperature for different external static magnetic fields H. As can be seen in the figure, χ' is suppressed by the magnetic field. As the field increases, the main peak of χ' decreases and a double-peak feature emerges. The ferrimagnetic phase-transition temperature determined from dc magnetization and specific heat is quite close to the position of the high-temperature peak in χ', which slightly increases with increasing field. The low-temperature peaks in χ' and χ'' correspond to the spin-glass transition. As the field increases, the low-temperature peak in χ' decreases and finally disappears under ~ 1 T (as shown in the inset). The peak in χ'' also shifts to lower temperature with increasing field. Under very high external field (above 1 T), the spin-glass transition seems to be completely suppressed.

The field versus temperature phase diagram obtained from this ac susceptibility measurement is shown in Fig. 8. Due to the large uncertainties associated with determining transition temperature of two nearby phase transitions, the error bars at low field are relatively large. However, the field dependence of the PM-FM transition is very weak in this region, while it is clear that the transition temperature gradually increases with increasing field at high fields. The spin-glass transition temperature, T_g, determined using the method described in Sec. III C, also exhibits substantial field dependence. Specifically, T_g is suppressed rapidly as external field larger than 200 Oe is applied. Below this threshold, T_g does not show a systematic change with the change in the field. According to

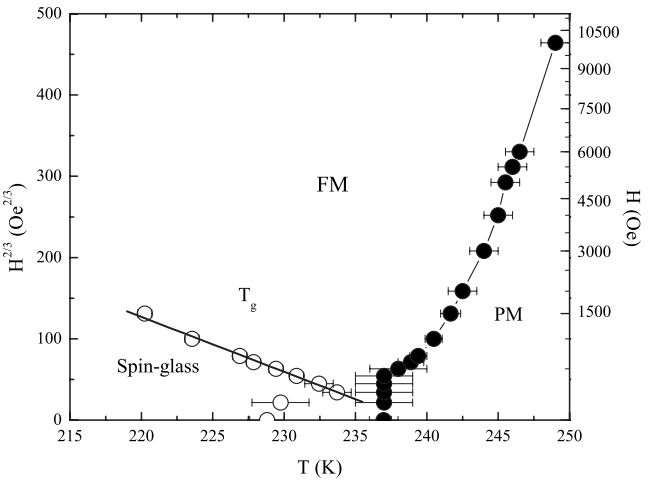

FIG. 8. Field vs temperature phase diagram. In order to show AT line, we plot $H^{2/3}$ versus T_g. The open and closed symbols denote the low- and the high-temperature transition temperatures as described in the text. The thick solid line is the linear fit to the AT line, Eq. (2), with $H_0=6.5$ T and $T_g(0)=239$ K.

the mean-field theory, there exists a phase boundary in H-T phase diagram called de Almeida-Thouless (AT) line,[36] whereby a spin-glass phase can only exist under this boundary (in the low-field region). The AT line is given by[36]

$$H = H_0\left(1 - \frac{T_g(H)}{T_g(0)}\right)^{3/2}. \quad (2)$$

Here H is the external magnetic field and $T_g(H)$ is the field-dependent glass transition temperature.[37] Our data fit this relation very well as shown in Fig. 8, in which a linear relationship between T_g and $H^{2/3}$ is clearly illustrated.

IV. DISCUSSION

We have presented several pieces of experimental evidence showing that the LFO sample goes through a spin-glass transition around 229 K. Before discussing the microscopic origin of the spin-glass behavior, it is useful to examine magnetic interactions. In LFO, both the Fe^{2+} and the Fe^{3+} ions are in their high spin configuration, with the spin angular momenta $S=2$ and $S=5/2$, respectively. The exchange interactions between Fe^{2+}-Fe^{2+} and Fe^{3+}-Fe^{3+} are presumably antiferromagnetic through the superexchange path via intervening oxygen ions, although recent calculation suggests that ferromagnetic Fe^{2+}-Fe^{2+} interaction is energetically very close to antiferromagnetic one.[38] However, the magnetic interaction between the Fe^{2+} and the Fe^{3+} ions requires further consideration. Note that the Fe^{2+} is in d^6 configuration and the Hund's rule dictates that the extra electron in this ion, compared to the $Fe^{3+}(d^5)$ ion, should point in the opposite direction of the rest of the "d^5" electrons. Therefore, one can expect the interaction between Fe^{2+} and Fe^{3+} to be ferromagnetic based on a kinetic-energy argument, analogous to the double exchange mechanism in manganites.[39] This argument is corroborated by the calculation in Ref. 38. However, since this compound is insulating at all tempera-

tures, such "extra" electron cannot be mobile but presumably resides in a resonance state between the two neighboring Fe ions. Therefore, it is quite conceivable that two neighboring Fe^{2+} and Fe^{3+} ions form a "dimer," sharing a minority-spin electron. In fact, such bond dimerization scenario has been considered in their study of mixed valence *B*-site Fe ions in Fe_3O_4 by Seo *et al.*[40] Further structural investigation of this system is required to address this speculation.

In general, disordered spin arrangements or interactions (random site or random bond) are necessary to produce magnetic frustration required for spin-glass behavior. The obvious source of such magnetic disorder in this sample is the oxygen nonstoichiometry. The TGA measurement reveals that about 0.07 additional oxygen per formula unit is present in our sample, implying that the ratio between the Fe^{3+} and the Fe^{2+} ions is roughly 4:3, which is comparable to other spin-glass system in terms of disorder concentration. For example, $Eu_xSr_{1-x}S_2$ is in the spin-glass ground state for $0.13 < x < 0.5$.[41] The uneven distribution of Fe^{3+}-Fe^{2+} ions most likely will alter local magnetic interactions. One can consider at least two ways this might happen. For example, in the above-mentioned bond dimerization picture, changing Fe^{2+} into Fe^{3+} will break up the dimer and create "impurity," spins which will introduce site disorder. However, it is also plausible that the nonstoichiometry fundamentally changes the property of charge ordering itself. Since the magnetic interaction between spins crucially depends on whether the ions involved is Fe^{3+} or Fe^{2+}, magnetic property is intimately related to the charge order. If the charge ordering at 300 K is not of the second-order kind, and has some relaxational component, such as charge-glass-type ordering, then this underlying glassy charge order will introduce bond disorder and might lead to spin-glass order. Detailed x-ray scattering studies are under way in order to elucidate complex temperature dependence of charge ordering in this compound.

We observe spin-glass phase transition that occurs within the ferrimagnetic-ordered phase. At this point, it is not clear whether this transition is accompanied by the destruction of ferrimagnetic long-range order (reentrant spin glass) or not. The possibility of coexistence of ferrimagnetic and spin-glass orders cannot be ruled out. Further neutron-scattering studies will be necessary to address this question. We also would like to note that the spin-glass transition temperature in this system is quite high compared to other well-known spin-glass systems. Our observation of spin-glass behavior at temperatures above 200 K is not only unusual but very surprising for a quasi-two-dimensional system since the lower critical dimension of Ising spin glass is believed to be two.[42] Again, these observations all indicate a quite unusual origin of the spin-glass behavior in this system.

V. SUMMARY

The magnetic properties of $LuFe_2O_{4+\delta}$ single crystals with excess oxygen ($\delta \sim 0.07$) were investigated with dc magnetization, ac susceptibility, and specific heat. Based on the dynamic scaling of ac susceptibility, nonequilibrium behavior such as aging and memory effects, it is suggested that $LuFe_2O_{4+\delta}$ goes through two phase transitions as a function of temperature. The high-temperature transition is a ferrimagnetic ordering at 237 K and the lower temperature transition at ~ 229 K is into a spin-glass phase. The field dependence of the spin-glass transition temperature is described well by the well-known de Almeida-Thouless theory. It was also observed that the ferrimagnetic transition temperature shows quite sizable field dependence. The possible role of oxygen nonstoichiometry as the microscopic origin for such spin-glass behavior has been discussed.

ACKNOWLEDGMENTS

We would like to thank David Ellis, S. M. Shapiro, G. Xu, J. Brittain, A. Gershon, and H. Zhang for invaluable discussions. The work at University of Toronto was supported by Natural Sciences and Engineering Research Council of Canada, Canadian Foundation for Innovation, Ontario Innovation Trust, and Early Researcher Award by Ontario Ministry of Research and Innovation. The work at Brookhaven was supported by the U.S. Department of Energy, Office of Science.

*yjkim@physics.utoronto.ca

[1] N. Kimizuka, E. Muromachi, and K. Siratori, *Handbook on the Physics and Chemistry of Rare Earths* (Elsevier Science, Amsterdam, 1990), Vol. 13, pp. 283–384.
[2] N. Kimizuka and T. Katsura, J. Solid State Chem. **13**, 176 (1975).
[3] W. C. Hamilton, Phys. Rev. **110**, 1050 (1958).
[4] J. García and G. Subías, J. Phys.: Condens. Matter **16**, R145 (2004).
[5] Y. Tomioka, A. Asamitsu, Y. Moritomo, H. Kuwahara, and Y. Tokura, Phys. Rev. Lett. **74**, 5108 (1995).
[6] Y. Yamada, N. Shinichiro, and N. Ikeda, J. Phys. Soc. Jpn. **66**, 3733 (1997).
[7] N. Ikeda, H. Ohsumi, K. Ohwada, K. Ishii, T. Inami, K. Kakurai, Y. Murakami, K. Yoshii, S. Mori, Y. Horibe, and H. Kitô, Nature (London) **436**, 1136 (2005).
[8] Y. Zhang, H. X. Yang, C. Ma, H. F. Tian, and J. Q. Li, Phys. Rev. Lett. **98**, 247602 (2007).
[9] H. J. Xiang and M.-H. Whangbo, Phys. Rev. Lett. **98**, 246403 (2007).
[10] S. Nagai, M. Matsuda, Y. Ishii, K. Kakurai, H. Kito, N. Ikeda, and Y. Yamada (unpublished).
[11] A. D. Christianson, M. D. Lumsden, M. Angst, Z. Yamani, W. Tian, R. Jin, E. A. Payzant, S. E. Nagler, B. C. Sales, and D. Mandrus, Phys. Rev. Lett. **100**, 107601 (2008).
[12] M. A. Subramanian, T. He, J. Chen, N. S. Rogado, T. G. Calvarese, and A. W. Sleight, Adv. Mater. **18**, 1737 (2006).
[13] For a review, see S. W. Cheong and M. Mostovoy, Nature Mater. **6**, 13 (2007), and references therein.
[14] J. Iida, M. Tanaka, Y. Nakagawa, S. Funahashi, N. Kimizuka,

and S. Takekawa, J. Phys. Soc. Jpn. **62**, 1723 (1993).
[15] M. Tanaka, M. Kato, N. Kimizuka, and K. Siratori, J. Phys. Soc. Jpn. **47**, 1737 (1979).
[16] M. Tanaka, J. Akimitsu, Y. Inada, N. Kimizuka, I. Shindo, and N. Siratori, Solid State Commun. **44**, 687 (1982).
[17] Y. Nakagawa, M. Inazumi, N. Kimizuka, and K. Siratori, J. Phys. Soc. Jpn. **47**, 1369 (1979).
[18] N. Ikeda, R. Mori, K. Kohn, M. Mizumaki, and T. Akao, Ferroelectrics **272**, 309 (2002).
[19] Y. Nakagawa, M. Kishi, H. Hiroyoshi, N. Kimizuka, and K. Siratori, *Ferrites*, Proceedings of the Third International Conference on Ferrites, Kyoto (CAPJ, Tokyo, 1981), p. 115.
[20] J. Iida, S. Takekawa, and N. Kimizuka, J. Cryst. Growth **102**, 398 (1990).
[21] J. Mattsson, T. Jonsson, P. Nordblad, H. Aruga Katori, and A. Ito, Phys. Rev. Lett. **74**, 4305 (1995).
[22] K. Gunnarsson, P. Svedlindh, J. O. Andersson, P. Nordblad, L. Lundgren, H. Aruga Katori, and A. Ito, Phys. Rev. B **46**, 8227 (1992).
[23] K. Gunnarsson, P. Svedlindh, P. Nordblad, L. Lundgren, H. Aruga, and A. Ito, Phys. Rev. Lett. **61**, 754 (1988).
[24] This functional form is often used in statistical analysis of extreme value distribution; see R. D. Reiss and M. Thomas, *Statistical Analysis of Extreme Values: With Applications to Insurance, Finance, Hydrology and Other Fields*, 3rd ed. (Birkhauser, Basel, 2007); however, we do not know why this fits our line shape at the moment.
[25] P. C. Hohenberg and B. I. Halperin, Rev. Mod. Phys. **49**, 435 (1977).
[26] R. Mathieu, D. Akahoshi, A. Asamitsu, Y. Tomioka, and Y. Tokura, Phys. Rev. Lett. **93**, 227202 (2004).
[27] J. A. Mydosh, *Spin Glass: An Experimental Introduction* (Taylor & Francis, London, 1993).
[28] E. Vincent and J. Hammann, J. Phys. C **20**, 2659 (1987).
[29] I. A. Campbell, Phys. Rev. B **37**, 9800 (1988).
[30] A. T. Ogielski, Phys. Rev. B **32**, 7384 (1985).
[31] A. T. Ogielski and I. Morgenstern, Phys. Rev. Lett. **54**, 928 (1985).
[32] K. H. Fischer and J. A. Hertz, *Spin Glasses* (Cambridge University Press, Cambridge, UK, 1991).
[33] L. Lundgren, P. Nordblad, P. Svedlindh, and O. Beckman, J. Appl. Phys. **57**, 3371 (1985).
[34] E. Vincent, V. Dupuis, M. Alba, J. Hammann, and J. P. Bouchaud, EPL **50**, 674 (2000).
[35] K. Jonason, E. Vincent, J. Hammann, J. P. Bouchaud, and P. Nordblad, Phys. Rev. Lett. **81**, 3243 (1998).
[36] J. R. L. de Almeida and D. J. Thouless, J. Phys. A **11**, 983 (1978).
[37] H. A. Katori and A. Ito, J. Phys. Soc. Jpn. **63**, 3122 (1994).
[38] M. Naka, A. Nagano, and S. Ishihara, Phys. Rev. B **77**, 224441 (2008).
[39] C. Zener, Phys. Rev. **82**, 403 (1951).
[40] H. Seo, M. Ogata, and H. Fukuyama, Phys. Rev. B **65**, 085107 (2002).
[41] H. Maletta and W. Felsch, Phys. Rev. B **20**, 1245 (1979).
[42] K. Binder and A. P. Young, Rev. Mod. Phys. **58**, 801 (1986).